Taylor & Francis
Taylor & Francis Group

RESEARCH ARTICLE

OPEN ACCESS | Check for updates

In vitro decidualisation of human endometrial stromal cells is enhanced by seminal fluid extracellular vesicles

Helena Rodriguez-Caro [a], Rebecca Dragovic [a], Mengni Shen [a], Eszter Dombi[a], Ginny Mounce [a], Kate Field[b], Jamie Meadows [b], Karen Turner [a,b], Daniel Lunn[c], Tim Child[a,b], Jennifer Helen Southcombe [a*] and Ingrid Granne [a*]

aNuffield Department of Women's & Reproductive Health, University of Oxford, Women's Centre, Oxford, UK; bOxford Fertility, Institute of Reproductive Sciences, Oxford, UK; cDepartment of Statistics, University of Oxford, Oxford, UK

ABSTRACT

Extracellular vesicles are highly abundant in seminal fluids and have a known role enhancing sperm function. Clinical pregnancy rates after IVF treatment are improved after female exposure to seminal fluid. Seminal fluid extracellular vesicles (SF-EVs) are candidate enhancers, however, whether SF-EVs interact with cells from the endometrium and modulate the implantation processes is unknown. Here, we investigated whether SF-EVs interact with endometrial stromal cells (ESCs) and enhance decidualisation, a requisite for implantation. SF-EVs, isolated from human seminal fluid ($n = 11$) by ultracentrifugation, were characterised by nanoparticle tracking analysis and Western blotting, and purified using size exclusion chromatography. Non-decidualised and decidualised primary ESCs ($n = 5$) were then treated with SF-EVs. Binding of bio-maleimide-labelled SF-EVs was detected by flow cytometry and fluorescence microscopy. Prolactin and IGFBP-1 protein levels in culture media were also analysed after single and multiple SF-EV exposure. SF-EVs size ranged from 50 to 300 nm, and they expressed exosomal markers (ALIX, SYNTENIN-1, CD9 and CD81). SF-EVs bound to non-decidualised and decidualised ESCs at similar levels. ESCs prolactin secretion was increased after single ($p = 0.0044$) and multiple ($p = 0.0021$) SF-EV exposure. No differences were found in IGFBP-1 protein levels. In conclusion, SF-EVs enhance *in vitro* ESC decidualisation and increase secretion of prolactin, an essential hormone in implantation. This elucidates a novel role of SF-EVs on endometrial receptivity.

Abbreviations: ECACC: European Collection of Authenticated Cell Cultures; ESCs: endometrial stromal cells; EVs: extracellular vesicles; FCS: foetal calf serum; HRP: horse-radish peroxidase; IFNγ: interferon-gamma; IGF: insulin-like growth factor; IGFBP-1: insulin-like growth factor binding protein 1; IVF: *in vitro* fertilisation; MVB: multivesicular bodies; NTA: nanoparticle tracking analysis; PRLR$^{-/-}$: homozygous prolactin receptor knockout; RT: room temperature; SF-EVs: seminal fluid extracellular vesicles; STR: short tandem repeat; TGFβ: transforming growth factor β; uNK: uterine natural killer

Introduction

Embryo implantation is a key limiting factor of *in vitro* fertilisation (IVF) success – only 36% of all transferred embryos in UK (2014) implant [1] and even the transfer of a day 5 embryo results in no more than a 50–60% implantation rate [2]. The "implantation window" of the menstrual cycle (days 20–24 of a 28-day cycle), occurs when the endometrium is receptive having undergone a phenotypic and functional transformation to support embryonic life. This process of decidualisation involves remodelling of the uterine vasculature and extracellular matrix, changes within the immune cell populations and phenotypic changes to endometrial epithelial cells and endometrial stromal cells (ESCs) [3] – characteristically the ESCs differentiate from a fibroblast-like morphology to enlarged round highly secretory cells. Prolactin and insulin-like growth factor binding protein 1 (IGFBP-1) are secreted by decidualised ESCs and are widely used as biochemical markers for stromal cell differentiation [4]. Prolactin is a polyfunctional hormone with an important role in reproduction [5–7]. Prolactin is synthesised by the endometrium at the beginning of decidualisation and prolactin levels rise until 20–25 weeks of pregnancy

---

and then decrease towards term [5]. IGFBP-1 is also essential in reproduction and, similar to prolactin, IGFBP-1 levels increase after the start of ESC decidualisation [8].

Several factors are known to regulate decidualisation, including seminal fluid – *in vitro* treatment of human decidualised ESCs with seminal fluid has been reported to raise prolactin and IGFBP-1 mRNA and protein levels [9,10]. A meta-analysis of clinical trials investigating the effect of seminal fluid exposure (either at the time of oocyte retrieval or embryo transfer) of the female reproductive tract on the pregnancy rate of IVF treatment showed significantly increased implantation rates ($p = 0.006$, risk ratio = 1.23, 95% CI) [11]. Seminal fluid contains not only sperm, but also androgens, such as testosterone [10], and soluble proteins such as transforming growth factor β (TGFβ) and interferon-gamma (IFNγ) that can interact with cells of the female reproductive tract [12]. Seminal fluid also contains highly abundant populations of extracellular vesicles (EVs). EVs are membrane enclosed complexes which facilitate cell–cell communication through their cargos, including proteins, lipids and nucleic acids (RNA and DNA). The main types of EVs are (i) exosomes – 30–100 nm vesicles formed in multivesicular bodies (MVB) and released into the intercellular space by fusion of the MVB with the plasma membrane, (ii) microvesicles – 100 nm–1 μm vesicles shed from the plasma membrane, (iii) apoptotic bodies – vesicles of approximately 1–5 μm, and (iv) large oncosomes – vesicles secreted by cancer cells [13,14]. In addition, there are many subtypes of EVs [15]. In the female reproductive tract, EVs are known to be in follicular fluid, amniotic fluid, endometrium and placenta [16]. In the male reproductive tract, EVs are produced by the male accessory sex glands, including the seminal vesicles and the prostate [17], and the epididymis (epididymosomes) [18], and are present in seminal fluid [17]. EVs produced by the prostate are internalised endocytic vesicles sizing from 40 to 500 nm and are known as prostasomes [19,20]. These EVs have been reported to promote sperm motility [21] and protect sperm against the female immune system [17]. Traditionally, scientists have denominated all EVs in the seminal plasma as prostasomes, but because these EVs are not exclusively produced by the prostate, nor do they all originate from endosomes, we refer to them here as seminal fluid extracellular vesicles (SF-EVs).

In this study, we have isolated and purified seminal fluid EVs and shown for the first time that SF-EVs bind to ESCs *in vitro* and enhance endometrial decidualisation. These results suggest a novel role of SF-EVs on endometrial receptivity.

Materials and methods

Isolation and culture of ESCs

Primary ESCs were isolated from endometrial biopsies obtained from patients at Oxford Fertility ($n = 3$) and the John Radcliffe Hospital, Oxford ($n = 3$) (ethical approval number #08/H0606/94). All patients gave written informed consent. Four patients had proven fertility and two were undergoing investigations for subfertility, patients were 38 ± 5 years of age at time of procedure.

Endometrial biopsies were mechanically digested and incubated with 1× liberase-TM (Roche, UK) and 50,000 U/ml of DNAse (Sigma-Aldrich, USA) for 30 min at 37°C. After incubation, the digest was passed through consecutive 70 μm and 40 μm filters (BD Biosciences, UK) to remove aggregates, and centrifuged at 300 × g for 3 min. ESCs were cultured in Dulbecco's modified Eagle's medium/Nutrient Mixture F-12 Ham (DMEM-F12) (Sigma-Aldrich, USA), supplemented with 10% foetal calf serum (FCS), penicillin (100 IU/ml), streptomycin (100 μg/ml) and 2 mM L-glutamine (Sigma-Aldrich, USA). Cells were cultured at 37°C, 20% O_2 and 5% CO_2. Culture media was changed every 2 days and cell passages were performed at ~80% of confluence. ESC decidualisation was induced supplementing the growth media with 0.5 mM dibutyryl cyclic-AMP sodium salt (Sigma-Aldrich, USA) and 1 μM progesterone (Sigma-Aldrich, USA). Decidualisation media was changed every 2 days and the treatment lasted for 7 days.

Culture of Ishikawa, St-T1b, and BeWo cells

Ishikawa cells (human endometrial adenocarcinoma cell line) [22] were obtained from Ms. Janet Carver (NDWRH, University of Oxford) and authenticated by the European Collection of Authenticated Cell Cultures (ECACC) in May 2017; the short tandem repeat (STR) DNA profile of our cells matched 100% with the ECACC Ishikawa cell profile. St-T1b cells (telomerase-immortalised human ESC line) [23] were obtained from Dr. Rupsha Fraser (MRC Centre for Reproductive Health, University of Edinburgh), and BeWo cells (human placenta choriocarcinoma cell line) [24] were provided by Dr. Gavin Collett (NDWRH, University of Oxford). These cells were cultured in DMEM-F12, supplemented with 10% FCS, penicillin (100 IU/ml), streptomycin (100 μg/ml) and 2 mM L-glutamine, at 37°C, 20% O_2 and 5% CO_2. Ishikawa cell decidualisation was performed as described for ESCs (above).

SF-EV isolation, purification and characterisation

Human seminal fluids were collected from patients at Oxford Fertility ($n = 11$). These patients were healthy men with normal sperm concentrations, whose age ranged from 28 to 47 years old (average age was 36 years old). Ethical approval was obtained for the South Central research board (ethical approval number #12/SC/0468). All patients gave written informed consent.

After collection seminal fluid samples were centrifuged at $1000 \times g$ for 10 min at room temperature (RT) then at $10,000 \times g$ for 10 min at RT to remove sperm. The supernatants were then collected and stored at −80°C before use. The supernatants were diluted into a total volume of 11 ml with PBS (Sigma-Aldrich, USA) and ultracentrifuged at $100,000 \times g$ for 2 h at 4°C using Beckman Coulter L-80 ultracentrifuge with a Sorval TH-641 swing out rotor (Beckman Coulter, UK). The pellets were resuspended in 500–1000 µl of PBS, equivalent to and determined by the starting volume of seminal fluid, and the SF-EV preparations were stored at −80°C until analysed by nanoparticle tracking analysis (NTA), electron microscopy or Western blotting or further purified to remove soluble proteins.

SF-EVs were further purified removing remaining soluble proteins using Exo-spin™ columns (Exo-spin™, Cell Guidance Systems, UK) – all binding and functional assays were performed with Exo-spin-purified SF-EVs; a modified protocol from Welton et al. [25] was followed. SF-EVs ($n = 11$) were pooled to create a more representative sample of the population. Briefly, 1000 µl of SF-EVs (post-centrifugation resuspended in PBS – from 11 patients) were added to pre-equilibrated columns (equilibration performed with PBS). SF-EVs were eluted with PBS under gravity collecting 30 fractions of 500 µl. The protein content of the fractions was determined by BCA protein assay and

their SF-EV concentration was determined by NTA. Purified fractions containing SF-EVs were pooled and stored at −80°C. For binding assays, pooled SF-EVs were incubated with 2 µM of the EV dye bio-maleimide (BODIPY FL N-(2-aminoethyl)-maleimide) (Table 1) for 30 min prior to Exo-spin™ SF-EV purification which removes excess dye. Bio-maleimide-labelled PBS was also purified with Exo-spin™ columns and used as negative control. In addition, purified pooled SF-EVs were analysed by electron microscopy to confirm absence of protein aggregates.

SF-EV characterisation

The concentration and size of SF-EVs were analysed by NTA using a NanoSight LM10 with a 405 nm laser (Malvern, UK). SF-EV preparations were diluted in PBS to reach concentrations inside the precision range of the NTA machine (2×10^8 to 10×10^8 particles/ml). EVs were measured at camera level 12 (camera shutter speed: 15 ms, camera gain: 350) using the following script: PRIME, DELAY 5, CAPTURE 60, REPEAT 5. Videos were analysed using NanoSight NTA 2.3 software (Malvern, UK). Protein content of SF-EVs was determined by BCA protein assay (Thermo Scientific, USA). In addition, SF-EVs were probed for exosomal markers by Western blot. Briefly, 10 or 5 µg of protein per sample was separated by electrophoresis using NuPAGE 4–12% Bis-Tris Gels (Life Technologies™, USA) under reducing conditions. Proteins were then transferred onto Immuno-Blot® PVDF Membranes (Bio-Rad, USA) using a BIORAD semidry Western blot apparatus and nonspecific binding was blocked with 5% milk in PBS. Membranes were then incubated overnight with primary antibodies towards ALIX, SYNTENIN-1, CD9, CD81 at 4°C (Table 1). Next, membranes were washed and incubated with appropriate secondary antibodies conjugated to horse-radish peroxidase (HRP) (Table 1).

Table 1. Fluorescence dyes, primary and secondary antibodies used for Western blot, flow cytometry and fluorescence microscopy.

Antibody/dye	Origin	Concentration/dilution	Antigen	Clones	Source
Western blotting					
Anti-ALIX IgG	Mouse	1/1,000	ALIX	3A9	Cell Signaling Technology, USA
Anti- CD9 IgG	Rabbit	1/1,000	CD9	EPR2949	Abcam®, UK
Anti-SYNTENIN-1 IgG	Rabbit	1/1,000	SYNTENIN-1	EPR8102	Abcam®, UK
Anti-TAPA 1 IgG	Rabbit	1/1,000	CD81	Polyclonal	Abcam®, UK
Anti-mouse-HRP	Goat	1/1,000	Mouse immunoglobulins	Polyclonal	Dako, Denmark
Anti-rabbit-HRP	Goat	1/1,000	Rabbit immunoglobulins	Polyclonal	Dako, Denmark
Flow cytometry/fluorescence microscopy					
Bio-maleimide (BODIPY FL N-(2-aminoethyl)-maleimide)		2 µM	Thiol groups		Molecular Probes, USA
Anti-β actin IgG	Mouse	1/500	β-actin	AC-15	Abcam®, UK
Anti-LC3	Rabbit	1/500	LC3	Polyclonal	MBL International, USA
Anti-Mouse IgG (Alexa Fluor® 594nm)	Donkey	1/200	Mouse immunoglobulin	Polyclonal	Molecular Probes, USA
Anti-Rabbit IgG (Alexa Fluor® 594nm)	Goat	1/200	Rabbit immunoglobulin	Polyclonal	Thermo Scientific, USA
DAPI		1/1,000	Nuclei		Molecular Probes, USA

Bands were developed using Pierce ECL Western blotting substrate (Thermo Scientific, USA).

Electron microscopy

10 µl of sample (bio-maleimide-labelled or non-labelled Exo-Spin^{TM} column purified SF-EVs) was applied to glow discharged carbon formvar 300 mesh Cu grids, and incubated for 2 mins. Grids were then quickly blotted and stained with 2% uranyl acetate (aqueous) for 10 s, blotted and air dried. Grids were imaged on a 120 kV FEI Tecnai12 TEM using a Gatan OneView digital camera.

SF-EV binding assays

All flow cytometry data in this paper were obtained using a BD LSRII flow cytometer (BD Biosciences, UK). 100,000 events were recorded per sample. The results were analysed using FACSDiva software version 8.0 (BD Biosciences, UK) and figures were created using FlowJo version 10 (Tree Star Inc., Ashland, USA).

Flow cytometry of Ishikawa cells

Bio-maleimide-labelled SF-EVs were incubated with Ishikawa cells at different SF-EVs quantities (2.5×10^{10}, 5×10^{10} and 10×10^{10} SF-EVs/10^6 cells) and incubation times (0.5, 1, 2 and 4 h) ($n = 3$). Cells were also incubated with the negative control (bio-maleimide-labelled PBS purified with Exo-spin^{TM} columns) or PBS alone. After incubation, cells were washed twice with PBS and lifted with accutase (Sigma-Aldrich, USA). Cells were then centrifuged for 5 s at $13,000 \times g$, resuspended in 500 µl of 2% FCS/PBS and analysed by flow cytometry.

Fluorescence microscopy and flow cytometry of ESCs, St-T1b and BeWo cells

Bio-maleimide-labelled SF-EVs were incubated with non-decidualised, day 3 and day 7 decidualised ESCs for 2 h at 37°C (5×10^{10} SF-EVs/10^6 cells) ($n = 3$) and analysed by flow cytometry. ESCs were incubated with the negative control (bio-maleimide-labelled PBS purified with Exo-spin^{TM} columns) or PBS alone. 2.5×10^5 ESCs were plated per well and an extra well was also used to quantify the number of cells at the different decidualisation stages. After the incubation, cells were washed twice with PBS and detached with accutase. Cells were centrifuged for 5 s at $13,000 \times g$. Pellets were resuspended in 500 µl of 2% FCS/PBS and analysed by flow cytometry.

Bio-maleimide-labelled SF-EVs were also incubated with non-decidualised and day 7 decidualised ESCs for 2 h at 37°C (5×10^{10} SF-EVs/10^6 cells) and analysed by

fluorescence microscopy; PBS was used as control. After SF-EV treatment, cells were washed thoroughly once with PBS, and fixed with 100% methanol (Sigma-Aldrich, USA) for 10 min at −20°C, washed, and permeabilised with 0.5% Triton X-100 (Sigma-Aldrich, USA) for 15 min at RT. Afterwards, cells were washed with PBS and incubated with murine antibodies towards β actin for 2 h at RT (Table 1) in permeabilisation buffer containing FCS (Thermo Fisher, USA). Then, cells were washed with PBS and incubated with polyclonal antibodies towards mouse IgG (Alexa Fluor® 594 nm) for 40 min at RT and with DAPI for 5 min at RT (Table 1). 20× and 40× fluorescence images were captured using IN Cell 1000 analyser (GE Healthcare Life sciences, UK).

Non-decidualised ESCs, St-T1b and BeWo cells were also treated with bio-maleimide-labelled SF-EVs for 2 h at 37°C (5×10^{10} SF-EVs/10^6 cells) and analysed by flow cytometry and fluorescence microscopy as described above. Cells were incubated with rabbit antibodies towards LC3 for 2 h at RT (Table 1), to define the cellular morphology, and polyclonal antibodies towards rabbit IgG (Alexa Fluor® 594 nm) were used (Table 1).

SF-EV functional studies

2.5×10^5 ESCs were plated per well. After 16 h, cells were treated with PBS (control group) or SF-EVs (SFEVs-1 and SFEVs-2 groups) (5×10^{10} SF-EVs/10^6 cells) for 2 h at 37°C. After incubation, cells were washed with PBS and decidualisation media was added. On day 3, cells were treated again with PBS (control and SFEVs-1 groups) or SF-EVs (SFEVs-2 group) (5×10^{10} SF-EVs/10^6 cells) for 2 h at 37°C. Non-treated wells were used to determine the number of cells present and calculate the amount of SF-EVs to add. After incubation, cells were washed again with PBS and incubated with new decidualisation media. Cell supernatants were collected and changed after 24 h for 7 days and the concentrations of prolactin and IGFBP-1 were determined by human prolactin ELISA (R&D systems, UK) and human IGFBP-1 ELISA (R&D systems, UK) kits following manufacturer's instructions. Prolactin and IGFBP-1 measures were performed in triplicate and duplicate, respectively. The results were normalised between patients.

Statistical analysis

Statistical significance in the SF-EV characterisations and the binding assays were determined using GraphPad Prism 7.01 (GraphPad Software, USA). Shapiro–Wilk

tests were used to confirm the normality of the data. Differences between SF-EV sizes before and after Exo-spin™ purification and between the negative control and the SF-EV-treated group in the binding assays were assessed by multiple Student's *t*-tests. Differences between the decidualisation stages in the SF-EVs group were determined using a repeated-measures one-way ANOVA with the Greenhouse–Geisser correction and a Tukey's multiple comparison test. Data were represented as mean ± SEM. Differences were significant if $p < 0.05$.

Statistical analysis of the functional studies was carried out using R3.3.2 (R Core Team, R Foundation for Statistical Computing, Austria). Prolactin and IGFBP-1 concentrations were modelled using the following logistic function, characterised by *Asym, xmid* and *φ*.

$$\sqrt[3]{Response} = \frac{Asym + a_1 z_1 + a_2 z_2}{1 + exp\left(\frac{xmid - Day}{\varphi}\right)}.$$

Asym represents the maximum asymptote of the curve, *xmid* is the position of the point of inflexion and *φ* is the scale parameter. The reference level was taken to be Control and z1 and z2 were indicator variables identifying the two treatments; thus, the parameters a1 and a2 provide estimates of the contrasts in maximum asymptote due to Treatment and can be formally tested for significance. For the model to be valid, it was necessary to ensure that the residuals were normally distributed and homoscedastic; this was achieved by taking the cube-root of the response variable for both Prolactin and IGFBP-1. With this transformation, both normal Q–Q plots and formal Shapiro–Wilk tests confirmed normality and plots of residuals against fitted values showed no indication of heteroscedasticity.

The data were multilevel in structure in that repeated measurements over time were recorded for each subject, so that it was necessary to take account of within-subject correlation in the statistical analysis. Therefore, multilevel non-linear models were fitted using the R-library *nlme* [26] with subject ID as level 1. Random effects were included across the parameters *Asym, xmid* and *φ*. When IGFBP1 was the response a likelihood-ratio test showed that reducing the parameterisation by dropping the random effect on *φ* had no effect on the quality of fit of the model (*p*-value = 0.9714).

Results

Characterisation and purification of SF-EVs

Semen samples were centrifuged at low speed to remove sperm, then SF-EVs were isolated by ultracentrifugation and their size and concentration were determined by NTA ($n = 11$). SF-EV concentrations varied between individual preparations ranging from 5×10^{11} to 6×10^{12} SF-EVs/ml (Supplemental Figure 1). The SF-EV size distribution profiles of the 11 samples were similar and SF-EVs between 50 and 350 nm were detected (Figure 1(a), detailed description in Supplemental Figure 1). The average modal size (defined as the most frequently occurring EV size) of SF-EVs was 116 ± 6 nm and the average SF-EV mean size was 144 ± 6 nm. The phenotype of the SF-EVs was determined by Western blotting. The exosomal protein markers ALIX, SYNTENIN-1, CD9 and CD81 were expressed in all the SF-EV samples ($n = 11$) (Figure 1(b)) – complete Western blot membranes are shown in Supplemental Figure 2, two gels were run and sample 1 was present on both to allow comparison of all of the 11 SF-EV preparations. SYNTENIN-1 was similarly expressed by the SF-EV samples, while ALIX and CD9 expression was more variable – for example, SF-EV samples number 5 and 11 showed higher expression of ALIX and CD9 while others were lower, 3 and 7. CD81 was detected in all samples but at varying levels, we noted higher CD81 expression (SF-EV samples 2, 4, 5, 7, 8, 9, 10, 11) than others (samples 1, 3 and 6).

SF-EVs isolated by ultracentrifugation were pooled and further purified using Exo-spin™ columns to remove residual seminal fluid proteins. SF-EVs from 11 specimens were pooled together and 30 fractions of 500 µl were collected from the Exo-spin™ column; SF-EV and protein concentrations of each fraction were then analysed by NTA and BCA protein assay (Figure 1(c)). The majority of SF-EVs were present in fractions 5–9. Proteins were eluted in two peaks; the first corresponded with SF-EVs in fractions 4–11 indicating vesicle bound proteins. The second peak (fractions 14–18) contained minimal numbers of EVs and was therefore likely to contain soluble seminal fluid proteins (Figure 1(c)). Fractions 5–9 were pooled together for further experiments. The average purification yield of SF-EVs using Exo-spin™ columns was 75% ($n = 4$). Non-purified pooled SF-EVs had an average mode size of 125 nm and an average mean size of 154 nm. Purified SF-EVs had an average mode size of 126 nm and an average mean size of 159 nm. No significant differences between SF-EV size before and after purification were observed (Figure 1(d)) ($n = 4$) and both of them expressed the same exosomal markers (ALIX, SYNTENIN-1, CD9 and CD81) (Figure 1(e)). Electron microscopy revealed SF-EVs ranging in size between 20 and 300 nm size with single and double membrane surfaces. Importantly, electron microscopy images showed minimal background protein and no widespread protein aggregation in non-labelled pooled SF-EVs (Figure 2(a)) or bio-maleimide-labelled pooled SF-EVs (Figure 2(b)).
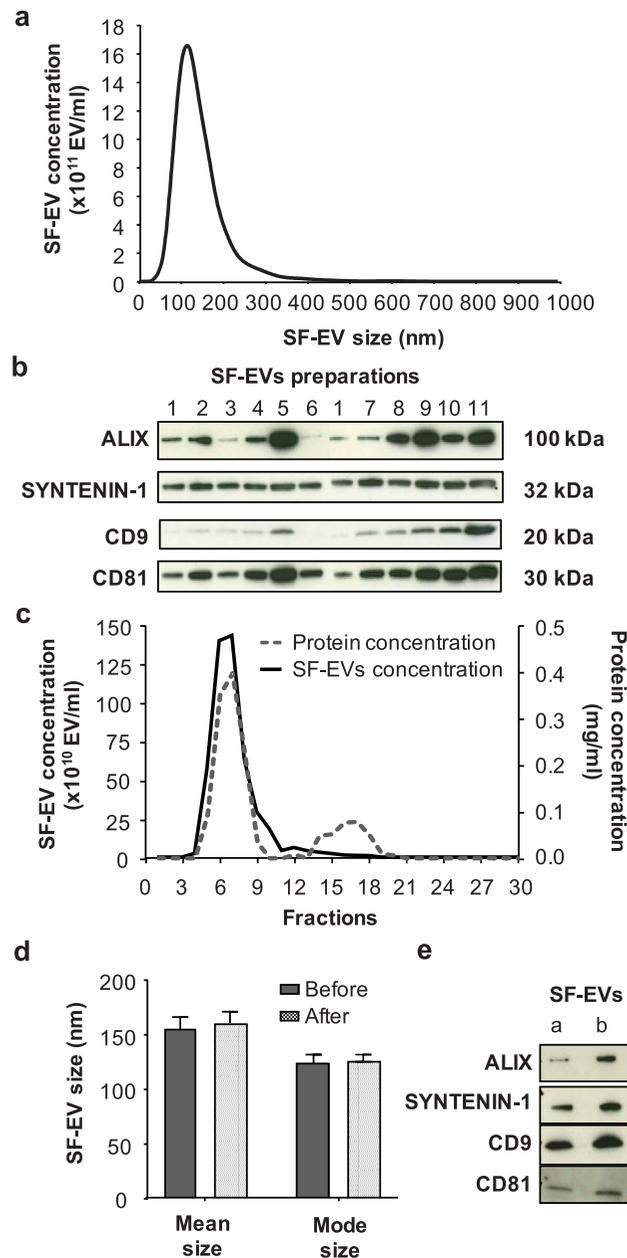
Figure 1. Characterisation and purification of SF-EVs. (a) Average size distribution of SF-EVs per sample ($n = 11$), analysed by nanoparticle tracking analysis (NTA) at camera level 12. (b) Western blot (10 µg) analysis of exosomal markers ALIX, SYNTENIN-1, CD9 and CD81 in SF-EV preparations ($n = 11$). (c) Purification of pooled bio-maleimide-labeled SF-EVs ($n = 11$) using Exo-spin^{TM} columns. SF-EVs were eluted with PBS and 30 fractions of 500 µl collected. Protein concentrations (dashed grey line) were determined using a BCA assay and SF-EV concentrations (solid black line) measured by NTA. (d) Mean and mode size of SF-EVs before and after Exo-spin^{TM} column purification. The samples were analysed by NTA. Bars represent mean ± SEM ($n = 4$). (e) Western blot (5 µg) analysis of exosomal markers ALIX, SYNTENIN-1, CD9 and CD81 in pooled SF-EVs before (a) and after (b) purification.

SF-EVs bind to primary ESCs in vitro

Fluorescent SF-EVs were generated by labelling with bio-maleimide, as previously described for syncytiotrophoblast EVs [27], this enables detection of EVs in association with cells by microscopy and flow cytometry. Titration and time course experiments using the endometrial cell line Ishikawa cells determined optimal SF-EV binding conditions (Supplemental Figure 3). 5×10^{10} bio-maleimide/SF-EVs were incubated with 10^6 primary ESCs for 2 h, then cells were washed, and analysed by flow cytometry and fluorescence microscopy to detect binding. To determine if SF-EVs had different binding affinities to ESCs depending on their stage of decidualisation, non-decidualised, day 3 and day 7 decidualised ESCs
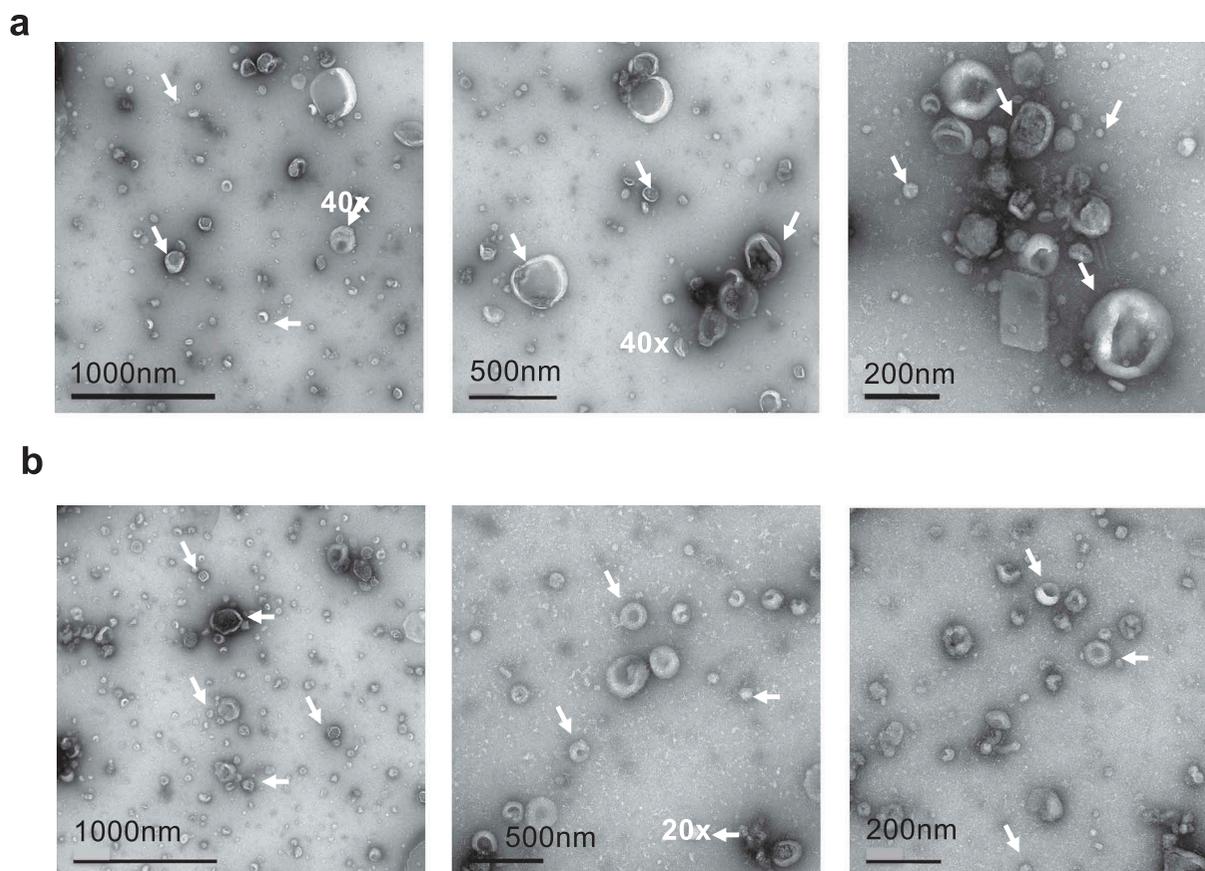
Figure 2. Electron microscopy images of SF-EV (a) non-labelled and (b) bio-maleimide-labelled pooled SF-EVs ($n = 11$) were analysed by transmission electron microscopy. SF-EVs between 20 and 300 nm in size were detected and protein aggregates were not found. Arrows mark SF-EVs detected in the samples.

were used. First, bio-maleimide/SF-EVs binding to ESCs was detected and quantified by flow cytometry ($n = 3$ ESC preparations) (Figure 3). A significant increase in mean FITC fluorescence intensity was detected when bio-maleimide/SF-EVs were incubated with ESCs on day 0 ($p = 0.012$), 3 ($p = 0.0251$) and 7 of decidualisation ($p = 0.0078$) compared to the PBS group (Figure 3(a–c)), a representative example of SF-EV binding above negative control (bio-maleimide-labelled PBS purified with Exo-spin™ columns) is shown in Figure 3(d). No increase in fluorescence was detected when comparing the negative controls with the PBS group (Figure 3(a–c)) and no significant differences in binding affinity were observed between different days of decidualisation. Secondly, fluorescence images revealed bio-maleimide-labelled SF-EVs (green) bound to non-decidualised (Figure 4(a)) and day 7 decidualised (Figure 4(b)) ESCs. No fluorescent signal was detected in the controls. SF-EVs bind preferentially to endometrial cells, including primary ESCs and St-T1b cells (immortalised ESC line) [23]. On the contrary, there was minimal binding of SF-EV to an irrelevant line of immortalised placenta choriocarcinoma, BeWo cells [24], shown

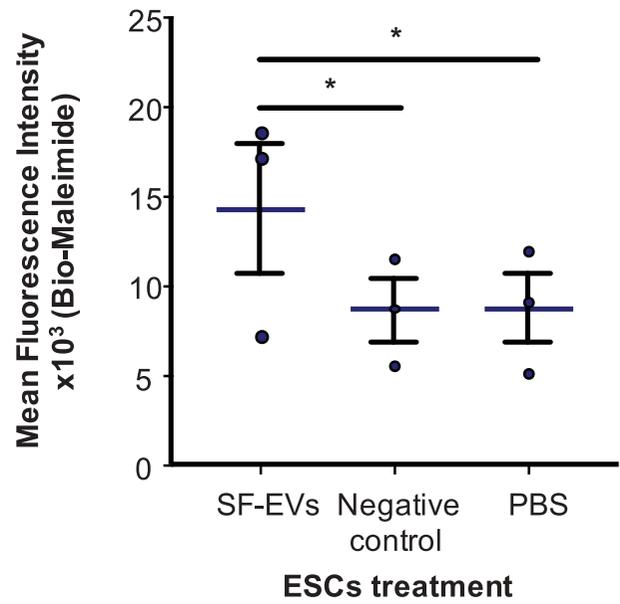by flow cytometry (Supplemental Figure 4) and fluorescence microscopy (Supplemental Figure 5).

SF-EVs promote prolactin but not IGFBP-1 secretion of primary ESCs in vitro

As SF-EVs associate with primary ESCs, we hypothesised SF-EVs might influence decidualisation. ESCs were treated with SF-EVs once for 2 h (day 0) then decidualised for 7 days. To test if multiple exposure to SF-EVs could further enhance endometrial receptivity cells were also treated with SF-EV on day 3 of decidualisation. Cell culture supernatants were collected and prolactin and IGFBP-1 secretion were analysed to identify variation in decidualisation between the treatments ($n = 5$). ESCs were cultured in the presence of 10% FCS and did not secrete prolactin prior to treatment. ESC prolactin secretion throughout time was significantly increased after single ($p = 0.0044$) and multiple ($p = 0.0021$) SF-EV treatment (Figure 5). Higher prolactin was detected from day 5 decidualisation after SF-EV treatment. No significant differences in prolactin
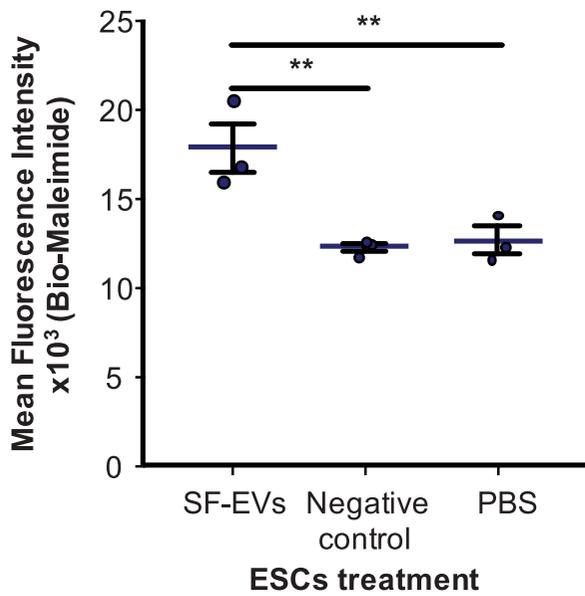
a Nondecidualised ESCs
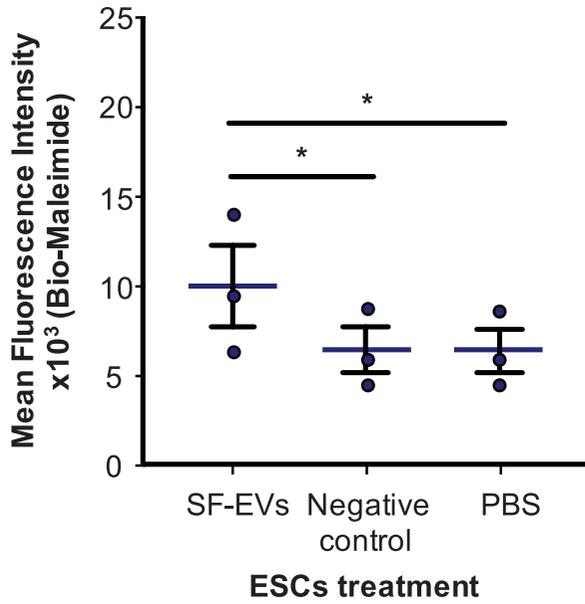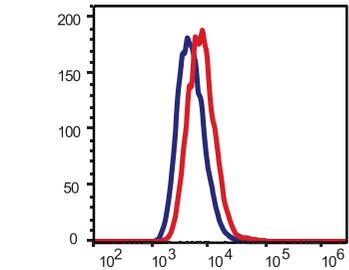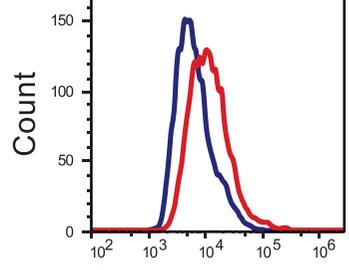

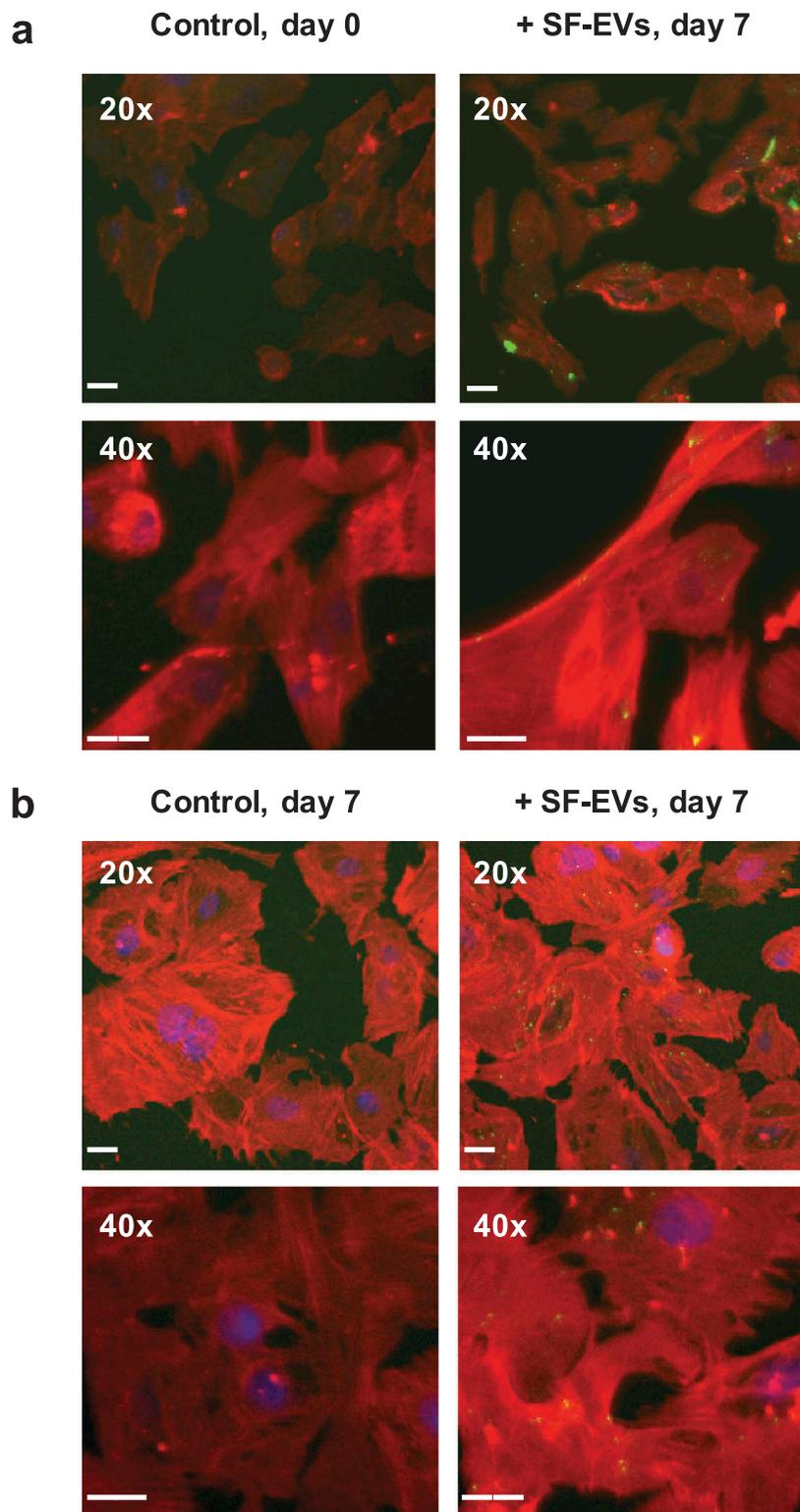## b Day 3 decidualised ESCs

c Day 7 decidualised ESCs

d
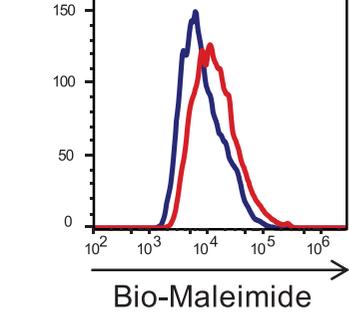
Figure 3. Flow cytometric analysis of SF-EV binding to primary ESCs (a) nondecidualised, (b) day 3 and (c) day 7 decidualised ESCs were incubated with bio-maleimide-labelled SF-EVs (5×10^{10} SF-EVs/10^6 cells), PBS or the negative control for 2 h and then analysed by flow cytometry. Bars represent mean ± SEM. *$p < 0.05$, **$p < 0.01$. (d) Representative flow cytometry histogram overlay image of SF-EV binding to primary ESCs on non-decidualised, day 3 and 7 decidualised ESC (blue line = PBS control; red line = + SF-EV).

Figure 4. Binding of SF-EVs to primary ESCs: Fluorescence microscopy (a) Non-decidualised and (b) day 7 decidualised ESCs were incubated with bio-maleimide-labelled SF-EVs (5×10^{10} SF-EVs/10^6 cells) and fluorescence images were captured at 20× and 40× magnification; green = SF-EVs, red = β-actin, blue = nuclei. Scale bars represent 20 μm.

secretion was observed between single and multiple SF-EV exposures ($p = 0.8128$) (Figure 5). Single ($p = 0.144$) and multiple ($p = 0.322$) SF-EV exposures did not change IGFBP-1 secretion by ESCs.

Discussion

We isolated SF-EVs ($n = 11$) sized between 50 and 350 nm by NTA, which is consistent with the size of prostasomes reported by Brody et al. [19]. Expression
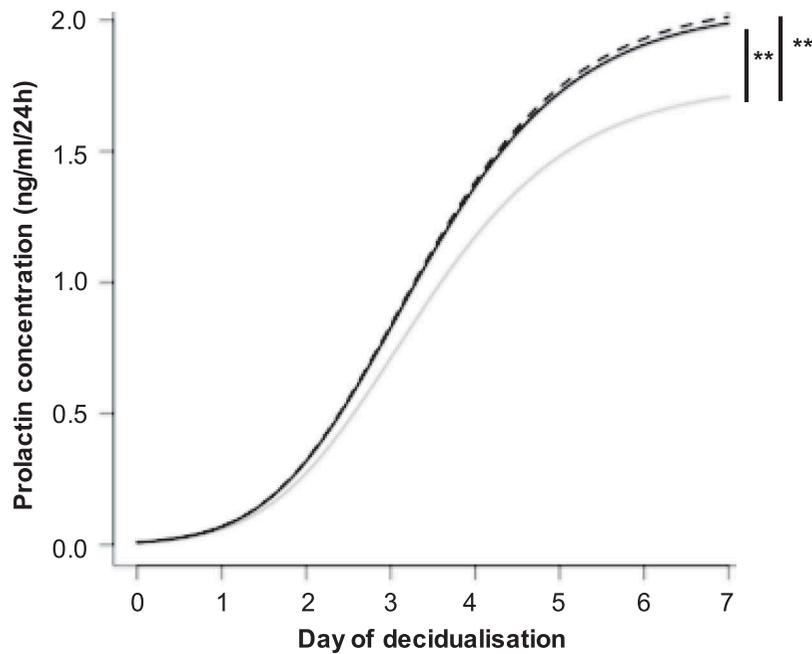
Figure 5. SF-EVs promote ESC decidualisation. Primary ESCs ($n = 5$) were treated with SF-EVs (5×10^{10} SF-EVs/10^6 cells) once (day 0 of decidualisation, solid black line) or twice (day 0 and 3 of decidualisation, dashed black line). Cells were treated with PBS in the control (solid grey line). (a) Prolactin concentration in cell supernatants at different SF-EVs exposures. $p < 0.05$ was considered significant. Prolactin secretion increased significantly after single (**$p = 0.0044$) and multiple (***$p = 0.0021$) SF-EV treatments throughout time.

of ALIX, SYNTENIN-1, CD9 and CD81 confirmed that some SF-EVs were exosomes. Microvesicles might also be present because the epididymis secretes this type of EV [17] – microvesicles are characterised by low expression of exosomal markers [16]. The variability in SF-EVs exosomal marker expression between patients might reflect differences in SF-EV populations, further analyses of these markers in a larger cohort than described here could help us to identify the SF-EVs biogenesis and release pathways involved [28]. Indeed, a larger study would enable correlation studies between SF-EV counts and clinical parameters and is merited. In addition, SF-EVs were further purified to remove non-EV associated seminal fluid proteins, which may have direct effect on ESCs. The purification was successful with an average 75% recovery yield, NTA and Western blotting confirmed SF-EV size and phenotype remained unaltered. Electron microscopy showed minimal background protein and no widespread protein aggregation in Exo-spin™ column purified SF-EVs. The latter is important in our experiments because protein aggregates can contain thiol groups and that would bind bio-maleimide, as described by Szabó-Taylor et al. [29]. Electron microscopy confirmed the sizing profiles of NTA, but also revealed the presence of vesicles smaller than 50 nm as previously observed by electron microscopy [20,30], which are beneath the detection limits of NTA.

In this study, we have shown for the first time that SF-EVs bind to primary human ESCs in vitro. SF-EVs were observed to bind similarly to non-decidualised, day 3 and day 7 decidualised ESCs in vitro suggesting that they can interact with the endometrium at similar intensity throughout the menstrual cycle. In addition, our data show SF-EVs enhance ESC decidualisation significantly inducing prolactin secretion. The importance of prolactin secretion for pregnancy is demonstrated by homozygous prolactin receptor knockout ($PRLR^{-/-}$) female mice, that are sterile because the maternal endometrium is refractive to embryo implantation [6]. As mentioned in the introduction, prolactin plays an important role in reproduction. In the endometrium, prolactin promotes ESCs decidualisation increasing progesterone receptors and its effects [31,32] and reduces myometrial contractions [33]. It also regulates endometrial epithelial cells by inducing expression of milk fat globule EGF factor 8 [34] and endometrial immune cells through interaction with uterine Natural Killer (uNK) cells; absence of prolactin limits uNK cells responsiveness to hypoxia and this leads to inadequate placental growth [35]. Prolactin also acts directly on placental cells and stimulates trophoblast migration and invasion [36]. Of importance here, we are aware that there are conflicting reports on the effects of serum on prolactin secretion of ESCs in vitro [37,38], as such we included controls and we

showed that in our model FCS had no effect on morphological decidualisation nor prolactin secretion.

Our data also showed that IGFBP-1, another decidualisation marker, was unchanged after SF-EV treatment. IGFBP-1 regulates insulin-like growth factor (IGF) I and II. During implantation, IGFBP-1 binds to trophoblast IGF-II with similar affinity as IGF-II receptor preventing excessive placental invasion, it also inhibits IGF-1 synthesis by ESCs [8]. The significant increase in prolactin, but not IGFBP-1, suggests that SF-EVs might preferably stimulate implantation processes regulated by prolactin but not IGFBP-1. Seminal fluid is known to promote the characteristic pro-inflammatory environment of pregnancy, reviewed by Robertson and Sharkey [39]. In mice, seminal fluid increases T regulatory cells in the endometrium [40], which could later suppress maternal immune response against paternal antigens. In humans (*in vitro* studies), seminal fluid induces endometrial secretion of several cytokines that play a role in implantation, such as granulocyte–macrophage colony-stimulating factor, interleukin 10 and macrophage inflammatory protein [41]. SF-EVs could be partially responsible for this effect through the enhancement of prolactin secretion by ESCs. The role of prolactin in the immune system has been extensively reviewed and it is known to supress or stimulate the immune responses in a dose-dependent manner [42,43]. For instance, low prolactin concentrations promote lymphocyte proliferation while high concentrations suppress it [44]. High levels of prolactin also inhibit cytotoxicity of uNK cells [45], which play an important role in cytokine secretion in the receptive endometrium.

Similar to this study, Doyle *et al.* showed that extended exposure (27 days) of decidualised ESCs to seminal plasma enhanced prolactin mRNA and protein levels [9]. Unlike this study, they also showed an increase in IGFBP-1 mRNA and protein levels. This difference may be due to the longer exposure to seminal plasma in their study (27 vs. 7 days) or due to the presence of other factors in the seminal plasma involved in ESC decidualisation, such as TGFβ-1 [46], relaxin [47], human chorionic gonadotropin [48], androgens such as testosterone [10], and prostaglandin E2 [49]. The mechanism underlying SF-EVs induction of prolactin by ESCs is unclear and future work needs to be undertaken to determine this. SF-EVs might transport proteins that stimulate ESC decidualisation. For instance, a previous study detected prostaglandin E in prostasomes although the concentration of this protein was low in comparison with soluble prostaglandin E and therefore unlikely to contribute a significant biological effect [50]. In addition, a proteomic study also detected TGFβ-2 in prostasomes [51] but it is unknown if TGFβ-2, akin to TGFβ-1 [46], can increase prolactin levels in the endometrium.

In this study, ESCs have been directly exposed to SF-EVs *in vitro. In vivo* it is likely that SF-EVs from the seminal plasma can reach the uterus and cross the mucosal epithelium. It has been shown that immotile-labelled particles deposited in the vagina are taken up into the uterus and oviducts in humans, probably by peristaltic movements [52]. In addition, sperm bind prostasomes at a neutral or slightly alkaline pH [17] and could transport them through the vagina and cervix on fertile days of the cycle. Prostasomes fuse with sperm under acidic conditions [17]. Afterwards, the SF-EVs would have to cross the epithelial barrier. Although there is no direct evidence for this in the endometrial epithelium, exosomes have been shown to cross the human intestinal epithelium [53] and the blood–brain barrier [54]. In the latter study, exosomes were transported primarily by transcytosis and, both caveolae-dependent, and clathrin-dependent endocytosis were involved [54].

In conclusion, we have shown that SF-EVs bind to ESCs *in vitro* and enhance prolactin secretion during the implantation window, which may improve the endometrial receptivity. It would be interesting to assess if SF-EVs could be used as a treatment in IVF.

Disclosure statement

No potential conflict of interest was reported by the authors.

ORCID

Helena Rodriguez-Caro http://orcid.org/0000-0003-3907-9660
Rebecca Dragovic http://orcid.org/0000-0002-4634-5165
Mengni Shen http://orcid.org/0000-0002-8866-2214
Ginny Mounce http://orcid.org/0000-0002-3219-8774
Jamie Meadows http://orcid.org/0000-0002-5238-6588
Karen Turner http://orcid.org/0000-0002-2117-7900

Jennifer Helen Southcombe http://orcid.org/0000-0003-0699-650X

Ingrid Granne http://orcid.org/0000-0002-7056-5723

References

[1] Authority HFAE. Fertility treatment 2014 - Trends and figures. 2016. p. 1–49 https://www.hfea.gov.uk/about-us/publications/

[2] Gardner DK, Surrey E, Minjarez D, et al. Single blastocyst transfer: a prospective randomized trial. Fertil Steril. 2004;81(3):551–555.

[3] Salamonsen LA, Nie G, Hannan NJ, et al. Society for reproductive biology founders' lecture 2009. Preparing fertile soil: the importance of endometrial receptivity. Reprod Fertil Dev. 2009;21(7):923–934.

[4] Dunn CL, Kelly RW, Critchley HO. Decidualization of the human endometrial stromal cell: an enigmatic transformation. Reprod Biomed Online. 2003;7 (2):151–161.

[5] Ben-Jonathan N, Mershon JL, Allen DL, et al. Extrapituitary prolactin: distribution, regulation, functions, and clinical aspects. Endocr Rev. 1996;17 (6):639–669.

[6] Bole-Feysot C, Goffin V, Edery M, et al. Prolactin (PRL) and its receptor: actions, signal transduction pathways and phenotypes observed in PRL receptor knockout mice. Endocr Rev. 1998;19(3):225–268.

[7] Marano RJ, Ben-Jonathan N. Minireview: extrapituitary prolactin: an update on the distribution, regulation, and functions. Mol Endocrinol. 2014;28(5):622–633.

[8] Fowler DJ, Nicolaides KH, Miell JP. Insulin-like growth factor binding protein-1 (IGFBP-1): a multifunctional role in the human female reproductive tract. Hum Reprod Update. 2000;6(5):495–504.

[9] Doyle U, Sampson N, Zenzmaier C, et al. Seminal plasma enhances and accelerates progesterone-induced decidualisation of human endometrial stromal cells. Reprod Fertil Dev. 2012;24(3):517–522.

[10] Narukawa S, Kanzaki H, Inoue T, et al. Androgens induce prolactin production by human endometrial stromal cells in vitro. J Clin Endocrinol Metab. 1994;78(1):165–168.

[11] Crawford G, Ray A, Gudi A, et al. The role of seminal plasma for improved outcomes during in vitro fertilization treatment: review of the literature and meta-analysis. Hum Reprod Update. 2015;21 (2):275–284.

[12] Bromfield JJ. Seminal fluid and reproduction: much more than previously thought. J Assist Reprod Genet. 2014;31(6):627–636.

[13] Raposo G, Stoorvogel W. Extracellular vesicles: exosomes, microvesicles, and friends. J Cell Biol. 2013;200(4):373–383.

[14] Minciacchi VR, Spinelli C, Reis-Sobreiro M, et al. MYC mediates large oncosome-induced fibroblast reprogramming in prostate cancer. Cancer Res. 2017;77 (9):2306–2317.

[15] Kowal J, Arras G, Colombo M, et al. Proteomic comparison defines novel markers to characterize heterogeneous populations of extracellular vesicle subtypes. Proc Natl Acad Sci U S A. 2016;113(8):E968–77.

[16] Tannetta D, Dragovic R, Alyahyaei Z, et al. Extracellular vesicles and reproduction-promotion of successful pregnancy. Cell Mol Immunol. 2014;11(6):548–563.

[17] Aalberts M, Stout TA, Stoorvogel W. Prostasomes: extracellular vesicles from the prostate. Reproduction. 2014;147(1):R1–14.

[18] Sullivan R. Epididymosomes: role of extracellular microvesicles in sperm maturation. Front Biosci (Schol Ed). 2016;8:106–114.

[19] Brody I, Ronquist G, Gottfries A. Ultrastructural localization of the prostasome - an organelle in human seminal plasma. Ups J Med Sci. 1983;88(2):63–80.

[20] Hoog JL, Lotvall J. Diversity of extracellular vesicles in human ejaculates revealed by cryo-electron microscopy. J Extracell Vesicles. 2015;4:28680.

[21] Park KH, Kim B-J, Kang J, et al. Ca2+ signaling tools acquired from prostasomes are required for progesterone-induced sperm motility. Sci Signal. 2011;4(173):ra31.

[22] Nishida M. The Ishikawa cells from birth to the present. Hum Cell. 2002;15(3):104–117.

[23] Samalecos A, Reimann K, Wittmann S, et al. Characterization of a novel telomerase-immortalized human endometrial stromal cell line, St-T1b. Reprod Biol Endocrinol. 2009;7:76.

[24] Bode CJ, Jin H, Rytting E, et al. In vitro models for studying trophoblast transcellular transport. Methods Mol Med. 2006;122:225–239.

[25] Welton JL, Webber JP, Botos L-A, et al. Ready-made chromatography columns for extracellular vesicle isolation from plasma. J Extracell Vesicles. 2015;4:27269.

[26] Pinheiro J, Bates DM. Mixed-effects models in S and S-PLUS. New York, Springer; 2000.

[27] Dragovic RA, Jha RK, Kumar V, et al. Multicolor flow cytometry and nanoparticle tracking analysis of extracellular vesicles in the plasma of normal pregnant and pre-eclamptic women. Biol Reprod. 2013;89(6):151.

[28] Hessvik NP, Llorente A. Current knowledge on exosome biogenesis and release. Cell Mol Life Sci. 2018; 75(2): 193–208.

[29] Szabó-Taylor, KE, Toth EA, Balogh AM, et al. Monocyte activation drives preservation of membrane thiols by promoting release of oxidised membrane moieties via extracellular vesicles. Free Radic Biol Med. 2017;108:56–65.

[30] Ronquist GK, Larsson A, Stavreus-Evers A, et al. Prostasomes are heterogeneous regarding size and appearance but affiliated to one DNA-containing exosome family. Prostate. 2012;72(16):1736–1745.

[31] Daniel JC Jr., Jetton AE, Chilton BS. Prolactin as a factor in the uterine response to progesterone in rabbits. J Reprod Fertil. 1984;72(2):443–452.

[32] Chilton BS, Daniel JC Jr. Differences in the rabbit uterine response to progesterone as influenced by growth hormone or prolactin. J Reprod Fertil. 1987;79 (2):581–587.

[33] Mati JK, Mugambi M, Muriuki PB, et al. Effect of prolactin on isolated rabbit myometrium. J Endocrinol. 1974;60(2):379–380.

[34] Franchi A, Bocca S, Anderson S, et al. Expression of milk fat globule EGF-factor 8 (MFG-E8) mRNA and protein in the human endometrium and its regulation by prolactin. Mol Hum Reprod. 2011;17 (6):360–371.

[35] Ain R, Dai G, Dunmore JH, et al. A prolactin family paralog regulates reproductive adaptations to a physiological stressor. Proc Natl Acad Sci USA. 2004;101(47):16543–16548.

[36] Stefanoska I, Jovanović Krivokuća M, Vasilijić S, et al. Prolactin stimulates cell migration and invasion by human trophoblast in vitro. Placenta. 2013;34(9):775–783.

[37] Luciano AA, Maslar IA, Kusmik WF, et al. Stimulatory activity of serum on prolactin production by human decidua. Am J Obstet Gynecol. 1980;138(6):665–669.

[38] Matsui N, Kawano Y, Nakamura S, et al. Changes in vascular endothelial growth factor production associated with decidualization by human endometrial stromal cells in vitro. Acta Obstet Gynecol Scand. 2004;83(2):138–143.

[39] Robertson SA, Sharkey DJ. Seminal fluid and fertility in women. Fertil Steril. 2016;106(3):511–519.

[40] Robertson SA, Guerin LR, Bromfield JJ, et al. Seminal fluid drives expansion of the CD4+CD25+ T regulatory cell pool and induces tolerance to paternal alloantigens in mice. Biol Reprod. 2009;80(5):1036–1045.

[41] McGuane JT, Watson KM, Zhang J, et al. Seminal plasma promotes lesion development in a xenograft model of endometriosis. Am J Pathol. 2015;185 (5):1409–1422.

[42] Pereira Suarez AL, López-Rincón G, Martínez Neri PA, et al. Prolactin in inflammatory response. Adv Exp Med Biol. 2015;846:243–264.

[43] Costanza M, Binart N, Steinman L, et al. Prolactin: a versatile regulator of inflammation and autoimmune pathology. Autoimmun Rev. 2015;14(3):223–230.

[44] Matera L, Cesano A, Bellone G, et al. Modulatory effect of prolactin on the resting and mitogen-induced activity of T, B, and NK lymphocytes. Brain Behav Immun. 1992;6(4):409–417.

[45] Gerli R, Rambotti P, Nicoletti I, et al. Reduced number of natural killer cells in patients with pathological hyperprolactinemia. Clin Exp Immunol. 1986;64 (2):399–406.

[46] Chang HJ, Lee JH, Hwang KJ, et al. Transforming growth factor (TGF)-beta1-induced human endometrial stromal cell decidualization through extracellular signal-regulated kinase and Smad activation in vitro: peroxisome proliferator-activated receptor gamma acts as a negative regulator of TGF-beta1. Fertil Steril. 2008;90(4 Suppl):1357–1365.

[47] Lane B, Oxberry W, Mazella J, et al. Decidualization of human endometrial stromal cells in-Vitro - Effects of progestin and relaxin on the ultrastructure and production of decidual secretory proteins. Hum Reprod. 1994;9 (2):259–266.

[48] Moy E, Kimzey LM, Nelson LM, et al. Glycoprotein hormone alpha-subunit functions synergistically with progesterone to stimulate differentiation of cultured human endometrial stromal cells to decidualized cells: a novel role for free alpha-subunit in reproduction. Endocrinology. 1996;137(4):1332–1339.

[49] Frank GR, Brar AK, Cedars MI, et al. Prostaglandin E2 enhances human endometrial stromal cell differentiation. Endocrinology. 1994;134(1):258–263.

[50] Oliw EH, Fabiani R, Johansson L, et al. Arachidonic acid 15-lipoxygenase and traces of E prostaglandins in purified human prostasomes. J Reprod Fertil. 1993;99 (1):195–199.

[51] Inder KL, Zheng YZ, Davis MJ, et al. Expression of PTRF in PC-3 Cells modulates cholesterol dynamics and the actin cytoskeleton impacting secretion pathways. Mol Cell Proteomics. 2012;11(2):M111.012245.

[52] Zervomanolakis I, Ott HW, Hadziomerovic D, et al. Physiology of upward transport in the human female genital tract. Ann N Y Acad Sci. 2007;1101:1–20.

[53] Vashisht M, Rani P, Onteru SK, et al. Curcumin encapsulated in milk exosomes resists human digestion and possesses enhanced intestinal permeability in vitro. Appl Biochem Biotechnol. 2017;183:993–1007.

[54] Chen CC, Liu L, Ma F, et al. Elucidation of exosome migration across the blood-brain barrier model In Vitro. Cell Mol Bioeng. 2016;9(4):509–529.